

Available online at www.sciencedirect.com

jmr&t
Journal of Materials Research and Technology
journal homepage: www.elsevier.com/locate/jmrt



Original Article

Performance of newly developed concretes incorporating WO_3 and barite as radiation shielding material



Hanan Al-Ghamdi ^a, M. Elsafi ^b, M.I. Sayyed ^{c,*}, Aljawhara H. Almuqrin ^a, P. Tamayo ^d

^a Department of Physics, College of Science, Princess Nourah Bint Abdulrahman University, P.O.Box 84428, Riyadh 11671, Saudi Arabia

^b Physics Department, Faculty of Science, Alexandria University, 21511 Alexandria, Egypt

^c Department of Physics, Faculty of Science, Isra University, Amman, Jordan

^d LADICIM (Laboratory of Materials Science and Engineering), University of Cantabria, E.T.S. de Ingenieros de Caminos, Canales y Puertos, Av./Los Castros 44, 39005 Santander, Spain

ARTICLE INFO

Article history:

Received 1 April 2022

Accepted 26 June 2022

Available online 30 June 2022

Keywords:

Radiation shielding of concrete

Heavyweight concrete

 WO_3

Radiation protection efficiency

ABSTRACT

The preparation of suitable materials with satisfactory nuclear and mechanical properties to shield the ionizing radiation is a major concern in design the radiation protection. In this work, a group of heavy concrete samples were prepared containing varying concentrations of Tungsten oxide, and the mechanical and radiation shielding properties of the resulting samples was studied using theoretical and experimental techniques. Good agreement between the experimental test and the theoretical data was confirmed at all examined energies. Using WO_3 in the present concretes increases the density of specimens as well as the photons shielding capability. The increase in the amount of WO_3 caused a reduction in the half value layer and an increase in the radiation protection efficiency for the prepared concretes. The linear attenuation coefficient (LAC) for the control concrete reduces from 0.665 to 0.127 cm^{-1} over the selected energy range, while it is reduced from 1.803 to 0.134 cm^{-1} and from 2.014 to 0.138 cm^{-1} for Conc-1 and Conc-2 samples. The mean free path results demonstrated that all the specimens with additive materials (i.e. WO_3 and barite) have lower MFP than the control concrete. Thus, incorporating WO_3 and barite into the concrete significantly decreases the MFP of the specimens. The high-density concrete (i.e. Conc-5) absorbs gamma photons more efficaciously than the lower density samples. The radiation protection efficiency (RPE) for Conc-5 is 99% at 0.122 MeV, which suggests that this concrete can stop almost all the incoming photons with low energy.

© 2022 The Author(s). Published by Elsevier B.V. This is an open access article under the CC BY-NC-ND license (<http://creativecommons.org/licenses/by-nc-nd/4.0/>).

* Corresponding author.

E-mail address: dr.mabualssayed@gmail.com (M.I. Sayyed).

<https://doi.org/10.1016/j.jmrt.2022.06.145>

2238-7854/© 2022 The Author(s). Published by Elsevier B.V. This is an open access article under the CC BY-NC-ND license (<http://creativecommons.org/licenses/by-nc-nd/4.0/>).

1. Introduction

Concrete was the first material utilized in construction around the world. It is used in the construction of all facilities due to its high efficiency, proper cost, and availability of its basic materials. It consists of a heterogeneous mixture of sand, cement, water, and one or more types of aggregate as well as other mineral materials. Concrete can be classified into three types based on its density: light, normal, and heavy [1]. The type of aggregate used in concrete production is one of the most important factors that influences its density. It is known that if the density of aggregates used in concrete is greater than 3000 kg/m^3 , it will produce concrete with a density greater than 2600 kg/m^3 , which can be classified as heavy concrete [2–6].

This century has witnessed a remarkable and significant advancement in the field of construction, and as a result, new types of concrete were developed for use in many important fields and applications in our daily lives, such as hospitals, homes, government facilities, military areas, and nuclear power plants [7]. Although concrete is used in all previous applications, specific types of concrete with specific characteristics must sometimes be selected based on the type of application in which the concrete will be used. For example, the properties of the concrete that is used to construct the walls of a nuclear reactor are vastly different from those used to construct a typical home or hospital containing radioactive materials. Thus, when planning to use concrete in the design of a specific facility, a set of physical, mechanical, and thermal properties of this concrete should be studied in order to determine the practicality of using this concrete [8–12]. In addition to these previously mentioned properties, the radiation protection properties of concrete that will be used in applications involving radioactive isotopes or radiation-emitting devices such as X-ray generators [11–13]. Lead has long been known as one of the most common materials used as a radiation shielding material. However, due to some of the disadvantages of lead (such as toxicity), building and construction engineers have attempted to find lead alternative materials with appealing radiation protection properties. Radiation Protection Concrete (RSC) is distinguished by its low cost, excellent radiation protection, long durability, and, most importantly, environmental friendliness [14,15]. Also, one of the advantages of RSC is that it can be designed to provide protection against both gamma rays and neutrons at the same time. In this case, RSC outperforms lead, which cannot effectively shield against neutrons well. In order for the RSC to be highly effective in radiation protection, its density must be relatively high so that the chance of interaction between incident photons with the concrete atoms increases, allowing this concrete to absorb the most photons and thus provide sufficient radiation protection [16]. Limestone aggregates must be replaced with specific heavy materials such as magnetite, barite, and hematite in order to increase the density of concrete. Several studies have found that using iron or steel raises the density of concrete to more than 5600 kg/m^3 [1,17].

The ability of concrete to provide sufficient protection against ionizing radiation is primarily depends on three

factors, which are radiation energy, concrete density, and the atomic number of concrete components. Increasing the energy of the photon increases its ability to penetrate from the medium (concrete), and thus in order to improve the efficiency of concrete to protect against high energy radiation, heavy materials (such as WO_3) must be used, which in turn increases the density of concrete and improves radiation protection properties [18,19]. It can be said that the use of heavy aggregates clearly increases the efficiency of concrete in radiation protection, so researchers in the field of developing radiation protection materials have focused on this aspect in designing different types of concrete for use in hospitals, radiation treatment rooms, nuclear power plants, and radioactive waste storage containers [20,21].

So far, many studies have been made on the radiation protection properties of different types of concrete with added certain types of heavy metals and glass oxides. Waly and Bourham [22] have studied the protective properties of a group of concrete samples of different compositions, and through the results obtained, they concluded that concrete containing 15.67% and 39.19% of PbO and Fe_2O_3 , respectively, has excellent radiation protection properties. In another study by Yao et al. [23] they have found that concrete containing Bi_2O_3 has higher attenuation factors than concrete containing PbO , due to the difference in density between the two samples prepared using PbO and Bi_2O_3 . Nikbin et al. [24] have studied the effect of both WO_3 and Bi_2O_3 (in nano-size dimensions) on the radiative attenuation properties of magnetite-containing concrete. The researchers have used a practical method using Cs-137 and Co-60 sources to measure the attenuation factors practically. And through the results, the researchers were able to understand the effect of increasing the heavy metal oxides WO_3 and Bi_2O_3 in nano-size dimensions on improving the attenuation properties of concrete. Recently, Gunoglu and Akkurt [2] have used the NaI detector and studied the radioactive attenuation factors of magnetite-containing concrete within the energy range of 511 and 1332 keV. The two researchers have found a perfect match between the practical results obtained in the laboratory with the theoretical results that they calculated using the XCOM program. The practical results obtained also showed that the linear attenuation factor is greatly dependent on the magnetite rate. The HVL results they obtained have showed that the concrete prepared using basalt-magnetite aggregate is better in terms of radial protection than normal concrete. Recently, Sukhpal Singh and Kanwaldeep Singh [25] have prepared green concrete containing hematite and studied the mechanical properties and radiation protection properties. By comparing their results with similar results for samples of normal concrete, the two researchers have found that green samples prepared using hematite are more efficient at blocking gamma radiation to a safe level. In another study by Aygün et al. [7], researchers have developed new types of heavy concrete containing a group of minerals and studied the protective properties from photons and neutrons. The researchers have made a comprehensive study of the shielding properties using three different techniques (theoretical study, practical experiment as well as simulation using Monte Carlo). Through the results they obtained, the researchers have showed that adding minerals to concrete leads to an

Table 1 – The oxide composition of Cement (CEM II 42.5).

Oxide Composition (%)									
	Al ₂ O ₃	SiO ₂	Fe ₂ O ₃	CaO	MgO	SO ₃	K ₂ O	Na ₂ O	L.O.I
Cement	4.88	21.38	5.86	58.22	2.66	2.87	0.32	0.41	3.40

improvement in its efficiency in absorbing photons, and thus a promising new concrete can be obtained to be used in radiation protection applications. Azeez et al. [26] have prepared samples of heavy concrete using steel slag, steel shot, and iron ore. The researchers have found that the radiation protection properties are significantly affected by the unit weight of the concrete mixtures. In continuation of the previous effort made by researchers to develop different types of heavy concrete, the researchers in this work have developed new concrete containing different percentages of WO₃, and the mechanical properties of the prepared samples have been studied. The radiative attenuation properties have been also studied using practical and theoretical techniques in order to determine the possibility of using the resulting concrete in radiation protection applications.

2. Materials and method

2.1. Materials

2.1.1. Cement

Portland cement (CEM II 42.5) was chosen in this work because it has distinctive properties such as its relative density 3.15, surface area is 3556 cm²/g, compressive strength 42.5 N/mm² and its soundness 1 mm. The oxide compositions was tabulated in Table 1 using EDX analysis (model JSM-5300 JEOL type) [27,28].

2.1.2. Aggregate

In this research, sand was used as fine aggregate and 20 mm diameter quarry stone as coarse aggregate. Barite was also used as a fine and coarse aggregate at the same time in a ratio of 1:3, respectively. To obtain heavier concrete, tungsten oxide was added while reducing the proportion of aggregate. The relative density and other physical properties of these aggregates were listed in Table .2 as well as the chemical composition of Sand, Stone and Barite were estimated using EDX analysis and tabulated in Table .3.

2.1.3. Chemical additives

F-type super-plasticizer (SP) related to ASTM C494 [29] was used during this work. Its relative density equal 1.2. This plasticizer was used to maintain slump stability in all prepared mixtures.

2.1.4. Concrete mix design

The mix designs were developed according to the C&CI Design Method based on ACI 211.1–91 [30]. The proportions of the mixture for a 1000 L mixture are shown in Table 4. The water to cement ratio is 0.5 for all prepared concretes where the proportions on the binder was 350 kg/m³ for all prepared mixtures. Barite was added by 200 kg/m³ for all prepared

mixtures. WO₃ powder was added by replacing the fine and coarse aggregate with proportions of 3%, 6%, 14%, 22% and 32%. The slump was maintained using the superplasticiser. Samples were cut with different thicknesses. Fig. 1 shows the prepared samples with constant in thickness.

2.2. Methodology

2.2.1. SEM test

Analysis of the microstructure of the mixtures was performed by using a scanning electron microscope (i.e., SEM) model JSM-5300 JEOL type to obtain a comprehensive characterization of the obtained mixtures.

2.2.2. Mechanical test

The compressive strength of concrete mixes was tested for 15 × 15 × 15 cm cubed samples after 28 days age, according to BS1881: Part 116 [31].

2.2.3. Shielding test

A high Pure Germanium detector (HPGe) was used to test the shielding efficiency of the investigated samples in The institute of Graduate Studies and Research, Alexandria University, Egypt [32,33]. Each concrete mix was tested for thicknesses of 1, 3 and 5 cm, with a fixed diameter of 8 cm. In the beginning, the detector was calibrated and then the initial count rate (N₀) was calculated in the absence of a concrete sample where the distance between the source and the detector was 24 cm, and then the sample to be tested for shielding efficiency with thickness (t, cm) and density (ρ, g/cm³) is placed between the detector and the source (see Fig. 2) to determine the count rate (N).

The mass attenuation coefficient (MAC) was experimentally determined from Eq. (1) [34]:

$$MAC = \frac{1}{t \times \rho} \ln \frac{N_0}{N} \tag{1}$$

The experimental results of MAC were compared with the XCOM results, where the MAC of the composite estimated by the next equation [10]:

$$MAC = \sum_i w_i (MAC)_i \tag{2}$$

Table 2 – Physical properties of present aggregates.

	Fine aggregate	Course aggregate	Barite
Relative density	2.59	2.63	4.20
Loose Unit Weight (t/m ³)	1.54	1.33	1.37
Hardness index	6.22	6.89	3.00
Fineness Modulus	2.31	–	1.22

Table 3 – Chemical compositions of the present Aggregates.

Oxides	Chemical Composition (wt%)		
	Fine aggregate	Coarse aggregate	Barite
SiO ₂	99.38	14.53	2.29
Al ₂ O ₃	–	0.72	0.31
Fe ₂ O ₃	–	0.41	0.13
CaO	0.01	42.85	0.04
MgO	–	2.18	0.15
SO ₃	0.04	0.03	–
K ₂ O	0.07	–	–
Na ₂ O	–	–	–
BaSO ₄	–	–	94.25
SrO	–	–	2.58
L.O.I	0.5	39.28	0.25

where, w_i , represent the weight fractions of the constituent elements. The linear attenuation coefficient (LAC) can be calculated by dividing the MAC on the sample density by the following equation [35]:

$$LAC = MAC \times \rho \quad (3)$$

The half and tenth value layers (HVL and TVL) are also calculated for the current samples by the following equation [36,37]:

$$HVL = \frac{LN(2)}{LAC}, TVL = \frac{LN(10)}{LAC} \quad (4)$$

The radiation protection efficiency (RPE) is determined using: [38]:

$$RPE, \% = \left[1 - \frac{N_1}{N_0}\right] \times 100 \quad (5)$$

3. Results and discussion

3.1. Density of mixtures

The density of the different prepared samples was determined by using the law $\rho = M(g) \times V(cm^3)$, where M and V is the mass and volume of the cylindrical concrete mix. From Fig. 3, it is clear that the density of the mixture increased with the increase in the percentage of WO_3 , it was found that the density increased from 2.34 g cm^{-3} to 2.72 g cm^{-3} and that's is due to the high density of tungsten oxide.

3.2. SEM results

The results of the SEM in Fig. 4 indicated that the tungsten oxide (WO_3) particles increased with an increase in its percentage in the prepared concrete, and the results showed that the WO_3 particles were very small rods compared to the quartz and barium particles found in Barite. From these microscopic morphological properties, it is clear that the higher the percentage of tungsten oxide, the more it penetrates into the voids in the mixture, and thus the porosity decreases, which gives an indication of the improvement of the mechanical and shielding properties.

3.3. Compressive strength results

The compressive strength is the most common and required property of concrete, which ensures the quality of concrete. Compressive strength test results are shown in Fig. 5. In general, it is evident that the addition of tungsten oxide has improved the compressive strength of concrete. This is because the size and shape of tungsten oxide plays a vital role in enhancing the interfacial area between the binder and the fine and coarse aggregates, which is the key to improving the compressive strength in addition to the high level of Barite in the mixture. In Fig. 4, replacing the WO_3 with 3%, 6%, 14%, 22% and 32% improved compressive strength by 2.70%, 4.00%, 8.00%, 8.22% and 8.32%, respectively, compared to the control mixture.

3.4. Gamma ray shielding results

The first step in the evaluation of the radiation attenuation features of the prepared concretes with different ratios of barite and WO_3 is to experimentally measured the mass attenuation coefficient (MAC) for the concrete sample without barite and WO_3 (called it the control concrete) and the other concretes with barite and WO_3 . The experimentally measured values are important parameter, because the authors can estimate other shielding quantities based on the experimental MAC values, so it is useful to test the accuracy of the measured MAC values, and this can be done by compare the measured values with theoretical values generated by XCOM software. In Table 5, the measured and XCOM values for the MAC of the control concrete and the concrete with barite and WO_3 were enlisted. In the same table, the uncertainty in the measured values as well as the relative deviation $\Delta(\%)$ between the experimental and XCOM results were listed. For the control concrete, a good

Table 4 – Concrete mix proportions.

Mix Name	Cement (kg.m ⁻³)	Sand (kg.m ⁻³)	Lime Stone (kg.m ⁻³)	Water (kg.m ⁻³)	Barite (kg.m ⁻³)	WO ₃ (kg.m ⁻³)	SP (kg.m ⁻³)
Control	350	850	950	175	–	–	6.8
Conc-1	350	800	800	175	200	50	7.2
Conc-2	350	750	800	175	200	100	6.9
Conc-3	350	700	750	175	200	200	8.1
Conc-4	350	650	700	175	200	300	7.8
Conc-5	350	600	650	175	200	400	7.6



Fig. 1 – Part of prepared samples for radiation shielding measurements with thickness 3 cm.

harmony between the experimental and XCOM data were observed. This is found at low and high energies. For 0.06 MeV, the measured MAC is 0.2795 cm²/g and this is close to 0.2844 cm²/g which is generated from XCOM. The Δ is 1.64%, while it is 2.33% at 0.81 MeV, 1.15% at 0.121 MeV and 3.84% at 1.408 MeV. If we look at the MAC for the

concretes with barite and WO₃, also a good harmony between the measured and XCOM values was saw, and the Δ (%) is small for all concretes, with a maximum Δ is found for Conc-1 and equal 5.12%. These agreement between the MAC obtained by the two mentioned methods for the control concrete and other concretes enable us to use the

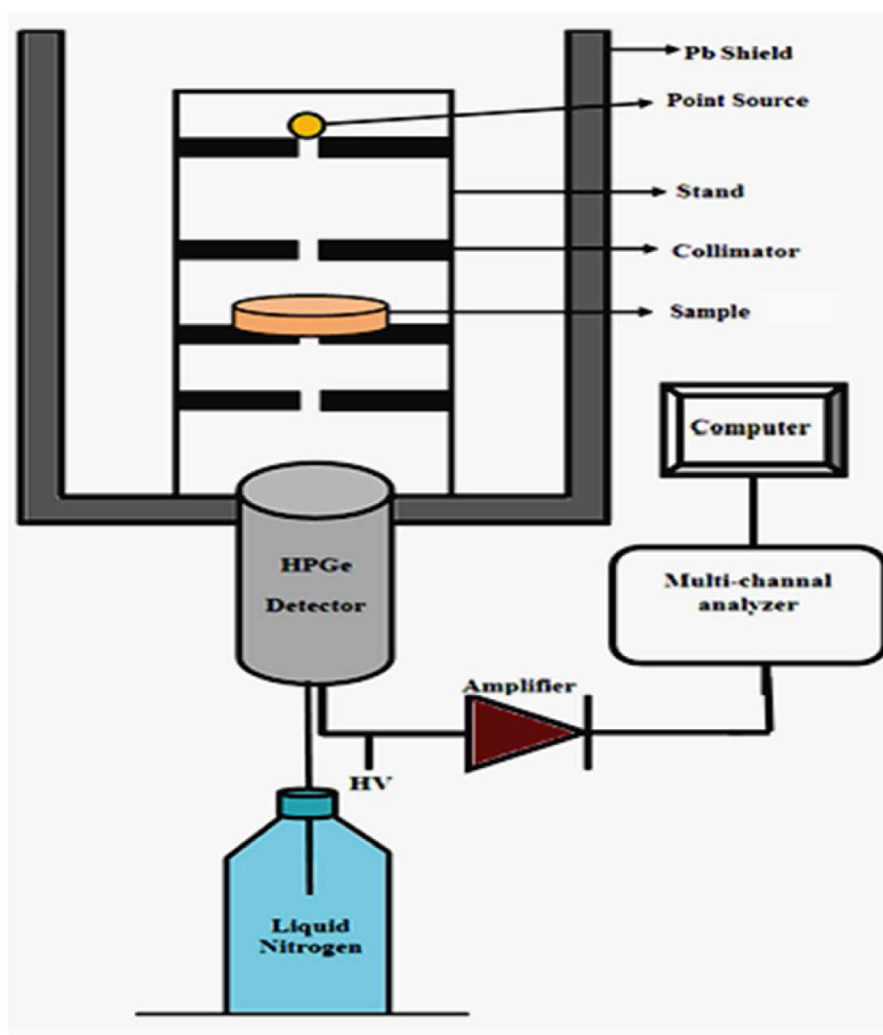


Fig. 2 – The illustration setup of the experimental work.

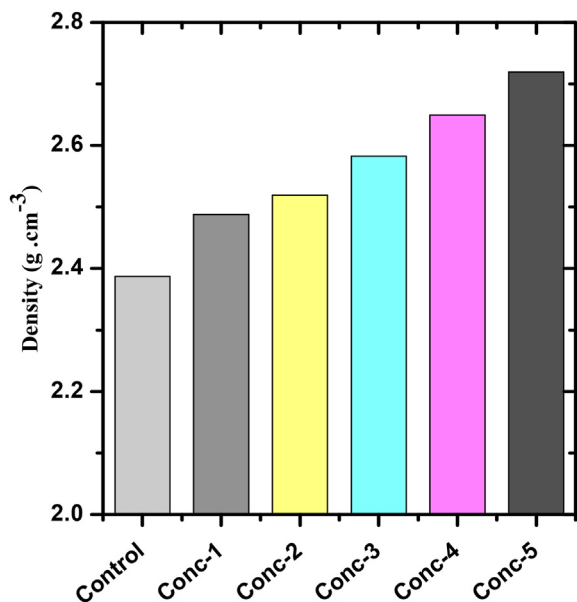


Fig. 3 – Density of concrete mixes.

experimental values for further calculations to determine the other shielding parameters for the investigated concretes.

Fig. 6 shows a graphical representation of the linear attenuation coefficient (LAC) as a function of the energy for the control concrete and the concretes with different ratios of barite and WO_3 . The LAC shows a decreasing with the energy and the shape of the curve is obey the general equation $N=N_0\exp(-LAC.x)$ which is known as Lambert–Beer law, so the change in the LAC with the energy has an exponential decay shape. The LAC for the control concrete reduces from 0.665 to 0.127 cm^{-1} over the selected energy range. Also, for the Conc-1 it is reduced from 1.803 to 0.134 cm^{-1} over the same energy range and from 2.014 to 0.138 cm^{-1} for Conc-2 sample. This exponential decay in the LAC for the prepared concretes describes the process of reducing the shielding ability rate for these concretes over a the selected energy range. On the other hand, the LAC for the control concrete is much lower than the LAC for the concretes with barite and WO_3 , especially at low energy. This means that the attenuation competence of these concretes with barite and WO_3 is better than that of the control concrete. On the other words, adding both barite and WO_3 causes an improvement in the attenuation competence for the concretes against gamma ray. Also, among Conc-1 to conc-5, the Conc-1 with highest amount of barite and zero content of WO_3 has lower LAC than Conc-2 to conc-5. While when moved from Conc-2 to conc-5 (the barite content is decreased and the WO_3 is increased) it was found that the LAC is increased and this is due to the replacement of the lower

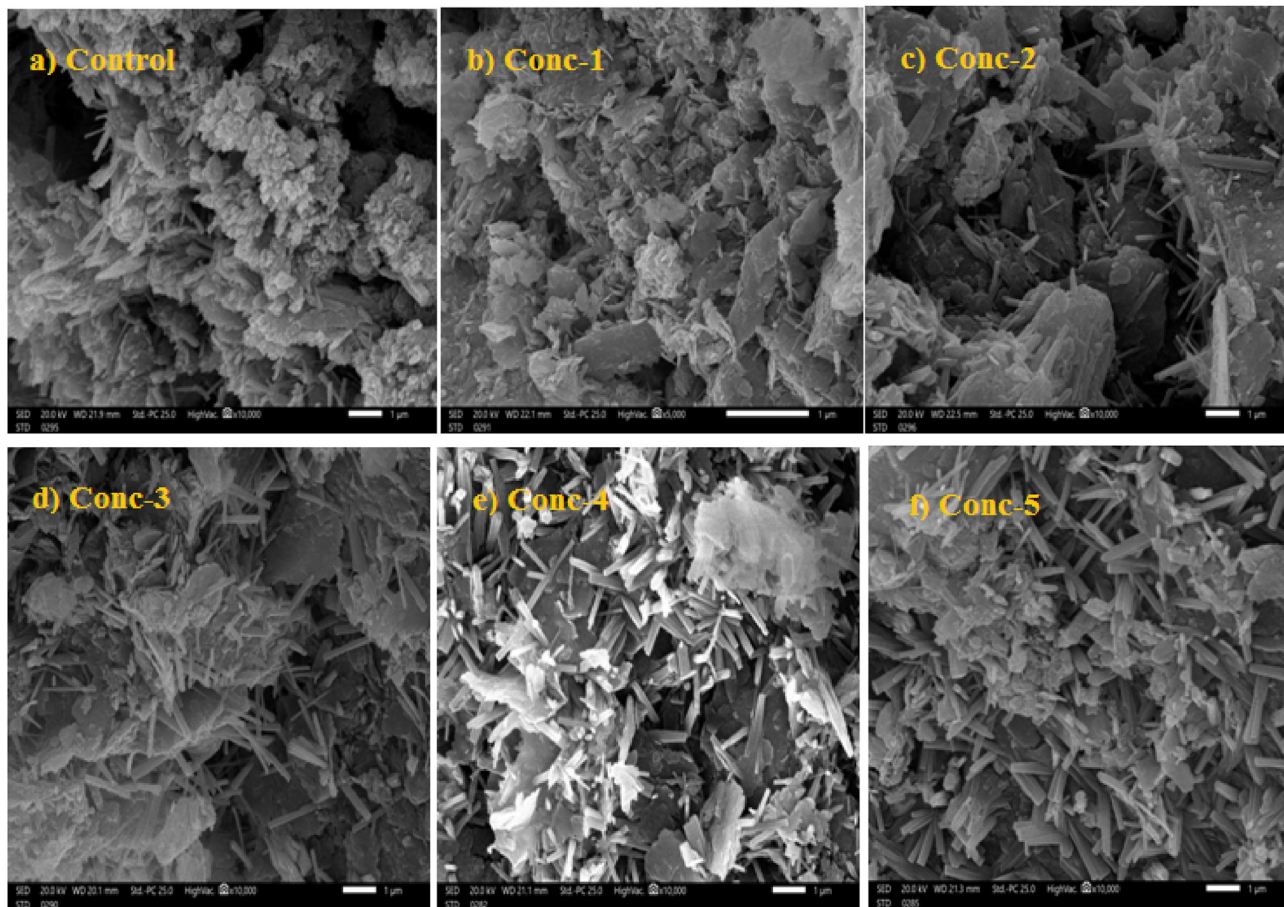


Fig. 4 – SEM images of prepared concrete mixes.

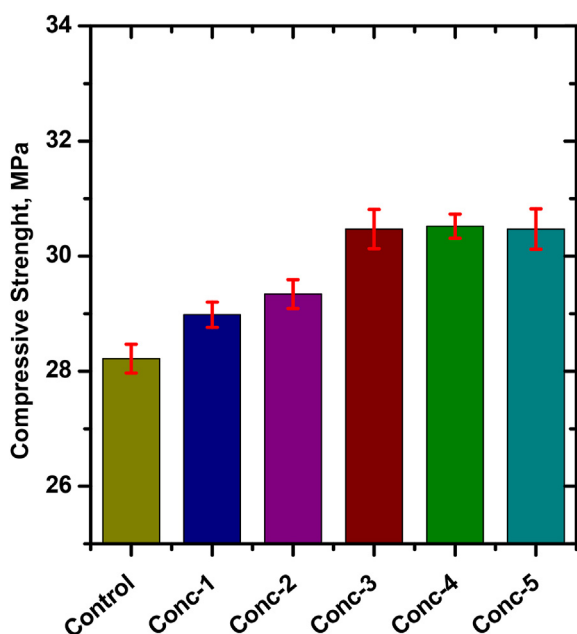


Fig. 5 – Compressive strength of prepared concrete mixes.

density compound (i.e barite, with a density of 4.48 g/cm³) with a higher density compound (i.e. WO₃, with a density of 7.16 g/cm³).

In order to check the dependency of the LAC on the WO₃, the LAC as a function of WO₃ contents at 0.345, 0.662 and 1.333 MeV was plotted (Fig. 7). Clearly, the LAC shows an increase behavior with adding WO₃ to the concretes. At 0.356 MeV, the LAC enhances from 0.238 cm⁻¹ (for control concrete), to 0.264, 0.290 and 0.330 cm⁻¹ for Conc-1, Conc-3 and Conc-5 respectively. This behaviour was correct at 0.662 and 1.333 MeV which confirms the linear relation between the amount of WO₃ presented in the concrete and the LAC values.

For the control concrete and the concretes with different concentrations of WO₃, the mean free path (MFP) as a function of the energy was investigated in Fig. 8-a, while in Fig. 8-b we studied the relation between the MFP with the WO₃ contents. The behavior of MFP is identical for all the prepared concretes due to the similarity in their chemical composition (with the difference only in the concentration of WO₃ and barite). The lowest MFP is occurred at 0.06 MeV and thereafter the MFP increased as the energy increased up to the highest tested photon energy. Such behavior is expected according to the inverse relation between the MFP and the LAC. The same

Table 5 – The experimental mass attenuation coefficient and its uncertainty as well as the relative deviation between the experimental and XCOM results.

Energy (MeV)	MAC, cm ² . g ⁻¹							
	Control				Conc-1			
	XCOM	EXP	UNC(EXP)	Δ(%)	XCOM	EXP	UNC(EXP)	Δ(%)
0.060	0.2844	0.2798	0.0005	1.64	0.7239	0.7511	0.0035	-3.62
0.121	0.1587	0.1569	0.0034	1.15	0.2562	0.2521	0.0008	1.63
0.245	0.1179	0.1124	0.0025	4.89	0.1310	0.1337	0.0009	-2.02
0.345	0.1017	0.1022	0.0014	-0.49	0.1059	0.1021	0.0025	3.72
0.662	0.0781	0.0791	0.0034	-1.29	0.0783	0.0752	0.0013	4.10
0.964	0.0655	0.0634	0.0028	3.26	0.0652	0.0622	0.0027	4.74
1.173	0.0594	0.0565	0.0036	5.12	0.0590	0.0581	0.0036	1.50
1.333	0.0556	0.0552	0.0042	0.80	0.0552	0.0542	0.0007	1.86
1.408	0.0541	0.0521	0.0009	3.84	0.0537	0.0529	0.0027	1.46
Energy (MeV)	Conc-2				Conc-3			
	XCOM	EXP	UNC(EXP)	Δ(%)	XCOM	EXP	UNC(EXP)	Δ(%)
0.060	0.7808	0.7959	0.0022	-1.90	0.8925	0.8831	0.0021	1.06
0.121	0.2989	0.2901	0.0014	3.03	0.3825	0.3931	0.0009	-2.70
0.245	0.1373	0.1348	0.0025	1.85	0.1496	0.1528	0.0027	-2.09
0.345	0.1081	0.1115	0.0007	-3.05	0.1125	0.1111	0.0036	1.26
0.662	0.0786	0.0779	0.0028	0.92	0.0793	0.0761	0.0015	4.19
0.964	0.0652	0.0639	0.0019	2.05	0.0653	0.0632	0.0029	3.37
1.173	0.0590	0.0591	0.0017	-0.24	0.0590	0.0564	0.0014	4.52
1.333	0.0552	0.0539	0.0005	2.39	0.0551	0.0538	0.0025	2.49
1.408	0.0536	0.0528	0.0018	1.59	0.0536	0.0533	0.0011	0.54
Energy (MeV)	Conc-4				Conc-5			
	XCOM	EXP	UNC(EXP)	Δ(%)	XCOM	EXP	UNC(EXP)	Δ(%)
0.060	1.0070	1.0329	0.0028	-2.51	1.1210	1.1392	0.0015	-1.60
0.121	0.4683	0.4517	0.0018	3.68	0.5539	0.5345	0.0024	3.63
0.245	0.1622	0.1589	0.0034	2.08	0.1747	0.1751	0.0037	-0.23
0.345	0.1169	0.1207	0.0019	-3.15	0.1214	0.1168	0.0009	3.94
0.662	0.0800	0.0789	0.0028	1.36	0.0807	0.0789	0.0017	2.23
0.964	0.0655	0.0657	0.0018	-0.38	0.0656	0.0651	0.0028	0.72
1.173	0.0589	0.0581	0.0013	1.45	0.0589	0.0579	0.0008	1.76
1.333	0.0551	0.0547	0.0011	0.71	0.0550	0.0539	0.0034	2.12
1.408	0.0535	0.0531	0.0014	0.81	0.0535	0.0531	0.0041	0.72

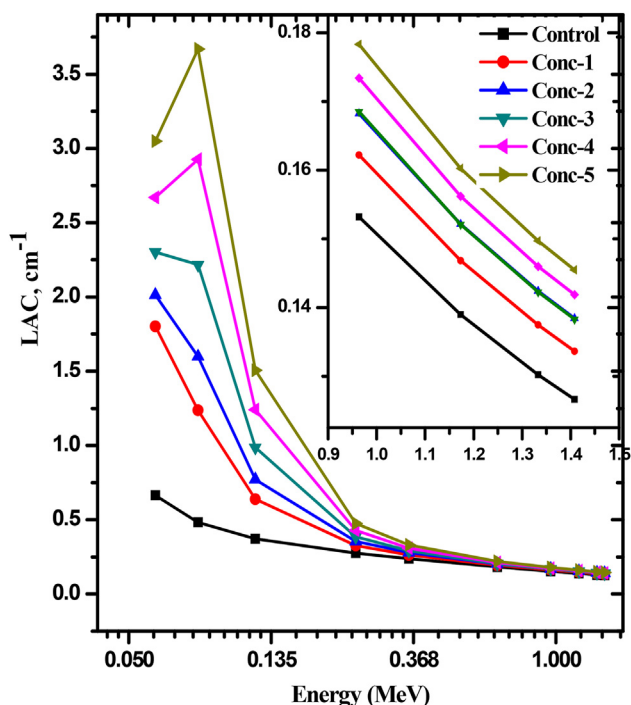


Fig. 6 – The LAC of different prepared concrete samples as a function of photon energy.

results were reported and discussed in more detail for other concretes and other shielding materials [39,40]. The results given in Fig. 8 demonstrate that the MFP is affected by the amount of WO_3 and barite in the concrete (additive materials).

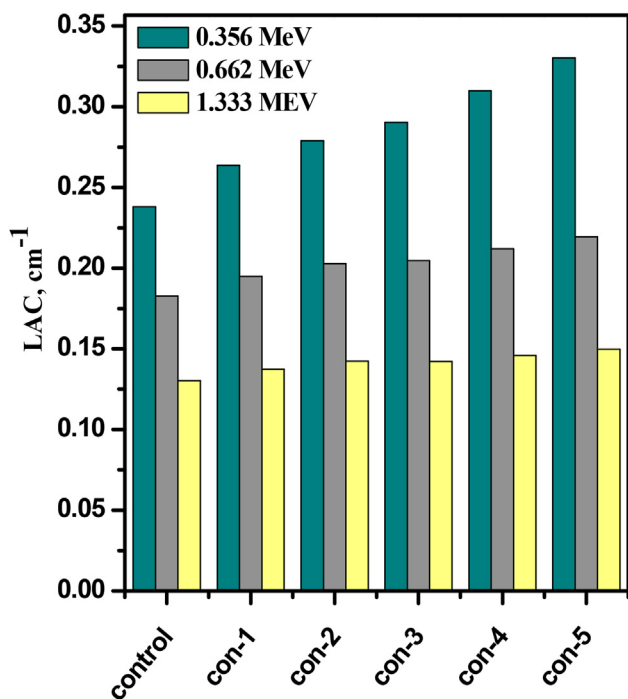


Fig. 7 – The LAC as a function of WO_3 contents at 0.345, 0.662 and 1.333 MeV.

If we look at control concrete (free WO_3 and barite) and Conc-1, the MFP of control concrete is higher than that of Conc-1. For example, at 0.06 MeV. Thus, incorporating WO_3 and barite into the concrete significantly decreases the MFP of the specimens. So, it was observed that all the specimens with additive materials (i.e. WO_3 and barite) have lower MFP than the control concrete. Now, Fig. 8-b compare the MFP for the Conc-1 to conc-5 and from this figure, it can examine the impact of WO_3 on the MFP for the prepared specimens. It was observed that adding WO_3 to the prepared specimens resulting in a notable decrease in the MFP of specimens. These findings suggest that incorporating the WO_3 in a concrete specimen can reduce the MFP and thus enhance the radiation protection performance. On the other words, the MFP decrease with the specimen density. Hence, the high-density concrete (i.e. Conc-5) absorbs gamma photons more efficaciously than the lower density samples.

For the control concrete and the concretes with different concentrations of WO_3 , it was investigated the HVL and TVL at some energise energy in Fig. 9-a and b. From this figure, it can examine the relation between the radiation shielding factors and the additive materials (WO_3 and barite). As it was found in the previous figure, the HVL and TVL are is low for higher density specimens, and the Conc-5 with highest density (due to the high amount of WO_3 in this specimen) has the lowest HVL as well as TVL. It is clear from Fig. 9 that changing the amount of WO_3 and barite affects the radiation attenuation factors. In addition to this observation, it was noticed that the rate at which the percentage of WO_3 and barite affects the HVL and TVL depends on the energy. The difference between HVL for Conc-1 and Conc-5 is 0.626 and 0.53 at low energies (i.e. 0.122 and 0.345 MeV), while it is 0.386 at 0.964 MeV. For the same two specimens, the difference between TVL at low energies is 2.08 and 1.769, while it is 1.28 at 9.964 MeV. At 0.122 and 0.345 MeV, Photoelectric effect is very important and this process highlghy depends on the atmc number of the shiels [41,42], so when added WO_3 to the prepared specimens, it was noticed that the amount of WO_3 had a noticeable effect on the HVL and TVL at these two energies.

One of the most important parameters in this work is the RPE. The importance of the RPE lies in the fact that it gives a direction indication about the possibility of using the prepared specimens in radiation shielding applications. Also, it gives information about the optimal concentration of WO_3 and barite in the prepared specimens that makes these specimens suitable for the radiation protection field. The RPE for our prepared specimens was examined in Fig. 10. It can easily notice that the RPE increases as the moving from Conc-1 to Concr-5, which indicates that incorporating WO_3 to the concrete has a positive impact on the RPE values. Also, it was found that the five specimens which contains different amounts of WO_3 and barite have higher RPE than the control concrete (the RPE for the control concrete is not shown in Fig. 10). The optimal amount of WO_3 that can improve the radiation protection performance for the present concretes is found in Concr-5, where the RPE for this specimen is 99% at 0.122 MeV, which suggests that this concrete can stop almost all the incoming photons with an energy of 0.122 MeV. For the same concrete, the RPE is 80% at 0.356 MeV, hence this concrete can stop most of the photons with an energy of

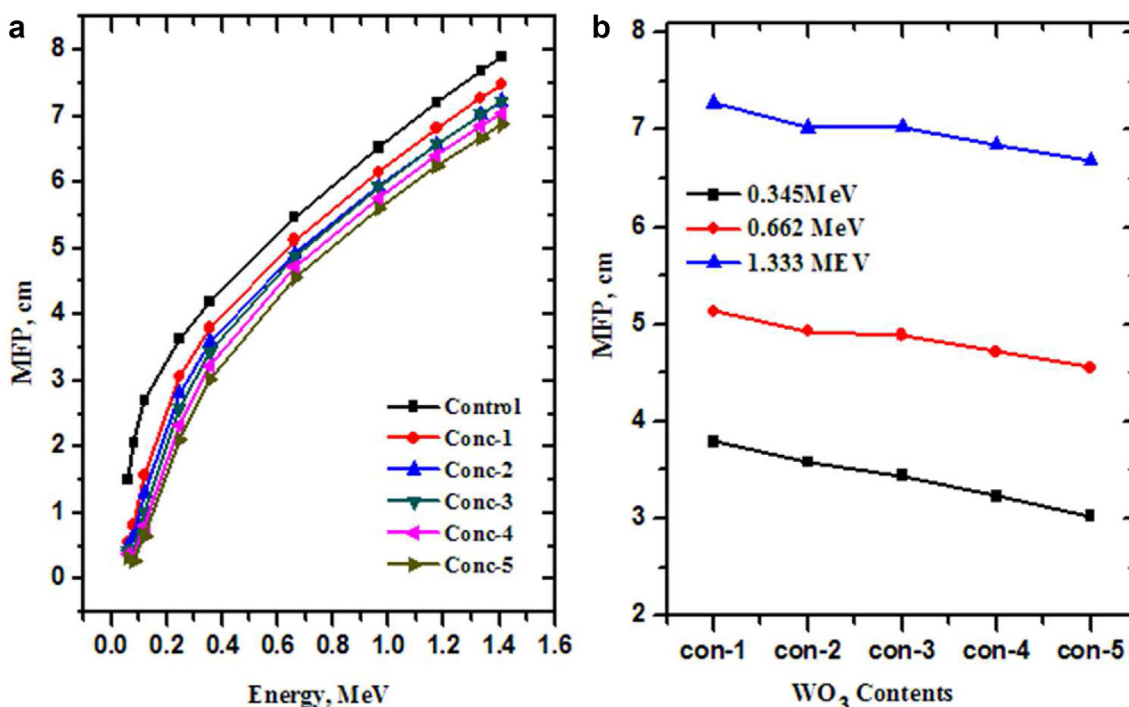


Fig. 8 – a) The MFP of different prepared concrete samples as a function of photon energy, b)The MFP as a function of WO₃ contents at 0.345, 0.662 and 1.333 MeV.

0.345 MeV and about 20% of the photons can penetrate Concr-5. For the same concrete (i.e. Concr-5), the RPE is 67% at 0.662 MeV, 59% at 0.964 MeV and 53% at 1.333 MeV.

Accordingly, Concr-5 with high concentrations of WO₃ is suitable concrete for radiation shielding in the range of 0.06–1.333 MeV. From Fig. 10 it was noticed that the RPE

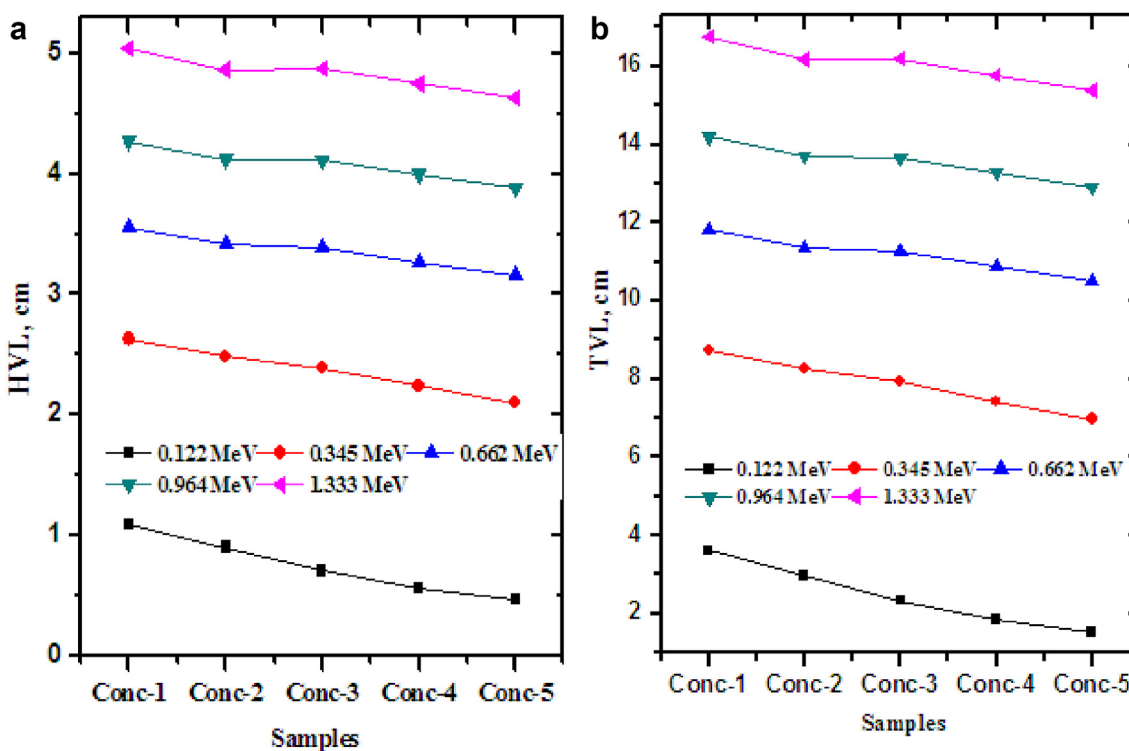


Fig. 9 – The half and tenth value layers (HVL and TVL) as a function of WO₃ contents at 0.122, 0.345, 0.662, 0.964 and 1.333 MeV.

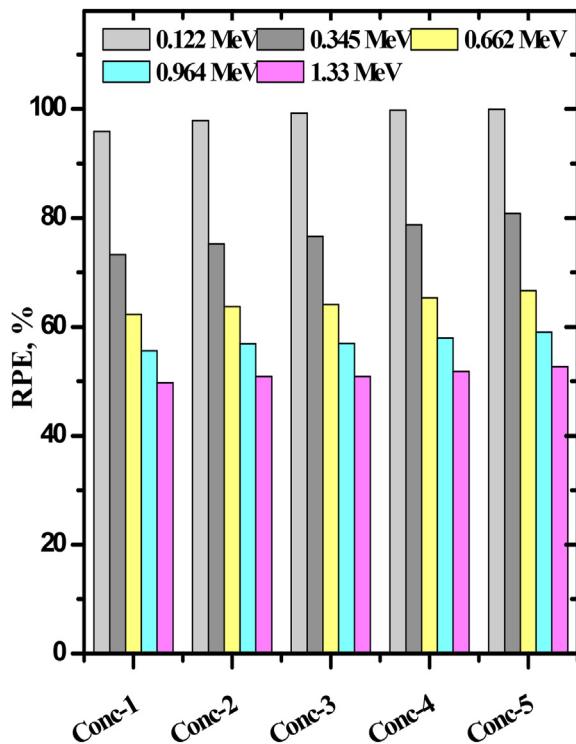


Fig. 10 – The RPE as a function of WO_3 contents at 0.122, 0.356, 0.662, 0.964 and 1.333 MeV.

decreases as the moving from 0.122 to 1.333 MeV. This means that the prepared concretes with WO_3 and barite have perfect attenuation performance when exposed to low energy photons.

The HVL for conc-4 and conc-5 was compared with MIII-0 (Ordinary concrete using CementIII), MIII-30H (30% of coarse aggregate was replaced by hematite) and MIII-30 S (30% of coarse aggregate was replaced by iron slag) as seen in

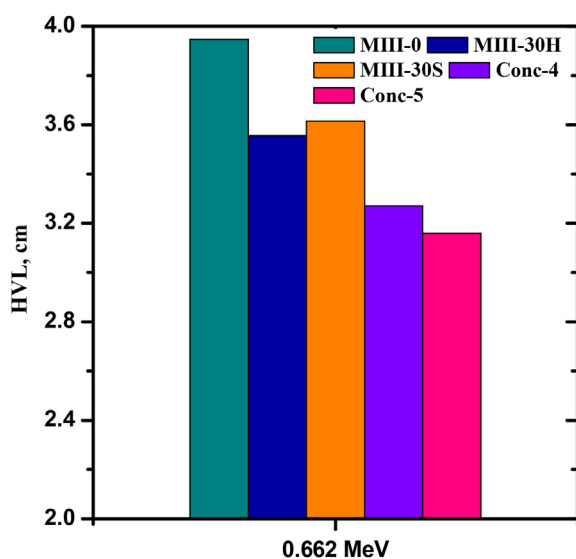


Fig. 11 – The half value layer for conc-4 and conc-5 in comparison with other shielding materials at 0.662 MeV.

Fig. 11. The HVL for conc-4 and conc-5 is lower than that of MIII-0, MIII-3-H and MIII-30 S and this is due to the high amounts of WO_3 presented in conc-4 and conc-5, which reaffirms the possibility of develop conc-4 and conc-5 for radiation protection field.

4. Conclusion

The authors aimed to assess the feasibility of using concrete with high amount of WO_3 for radiation shielding applications. The LAC, MFP and RPE values were utilized to quantify the impact of WO_3 and barite on the attenuation performance for the concrete samples. The results demonstrated that using high amount of WO_3 is a practical approach to develop a new concrete with interesting radiation protection performance. Experimental results appeared that the At 0.345 MeV, the LAC enhances from 0.238 cm^{-1} (for control concrete), to 0.264, 0.290 and 0.330 cm^{-1} for Conc-1, Conc-3 and Conc-5 respectively. The amount of WO_3 is also affected the HVL and TVL, but the influence of WO_3 on both parameters is notable at low energy, where the difference between HVL for Conc-1 and Conc-5 is 0.626 and 0.53 at low energies (i.e. 0.122 and 0.345 MeV), while it is 0.386 at 0.964 MeV. The RPE for Conc-5 with highest WO_3 was better than the control concrete and other concretes (i.e. con 1- to con-4), thus Conc-5 is suitable for radiation shielding.

Declaration of Competing Interest

The authors declare that they have no known competing financial interests or personal relationships that could have appeared to influence the work reported in this paper.

Acknowledgment

The authors express their gratitude to Princess Nourah bint Abdulrahman University Researchers Supporting Project number (PNURSP2022R28), Princess Nourah bint Abdulrahman University, Riyadh, Saudi Arabia.

REFERENCES

- [1] Ouda AS. Development of high-performance heavy density concrete using different aggregates for gamma-ray shielding. *Prog Nucl Energy* 2015;79:48–55.
- [2] Gunoglu Kadir, Akkurt Iskender. Radiation shielding properties of concrete containing magnetite. *Prog Nucl Energy* 2021;137:103776.
- [3] Martinez-Barrera G, Menchaca-Campos C, Gencel O. Polyester polymer concrete: effect of the marble particle sizes and high gamma radiation doses. *Construct Build Mater* 2013;41:204–8.
- [4] Baalamurugan J, Kumar VG, Chandrasekaran S, Balasundar S, Venkatraman B. Utilization of induction furnace steel slag in concrete as coarse aggregate for gamma radiation shielding. *J Hazard Mater* 2019;369:561–8.
- [5] Santhakumar AR, Chandrasekaran S, Viswanathan S, Mathiyarasu R, Venkatraman B. Effect of heat treatment on

- neutron attenuation characteristics of high density concretes (HDC). *Prog Nucl Energy* 2016;93:76–83.
- [6] Gholampour A, Gencil O, Ozbakkaloglu T. Physical and mechanical properties of foam concretes containing granulated blast furnace slag as fine aggregate. *OH Oren. Construct Build Mater* 2020;238:117774.
- [7] Hiremath Parameshwar N, Thanu Habbale Puttaraju, Basavana Gowda Sangahalli Nagaraja, Goudar Sharan Kumar. Early-strength development of blended concrete under different curing conditions. *Emerg Mater Res* 2020;9(1):59–64.
- [8] Gökç HS, Canbaz-Öztürk B, Çam NF, Andiç-Çakır Ö. Gamma-ray attenuation coefficients and transmission thickness of high consistency heavyweight concrete containing mineral admixture. *Cement Concr Compos* 2018;92:56–69.
- [9] Gökçe HS, Yalçinkaya Ç, Tuyan M. Optimization of reactive powder concrete by means of barite aggregate for neutrons and gamma rays. *Construct Build Mater* 2018;189:470–7.
- [10] Sayyed MI, Hamad M Kh, Mhareb MHA, Kurtulus Recep, Dwaikat Nidal, Saleh Marwa, et al. Assessment of radiation attenuation properties for novel alloys: an experimental approach. *Radiat Phys Chem* 2022;110152.
- [11] Aygün B, Sakar E, Agar O, Sayyed MI, Karabulut A, Singh VP. Development of new heavy concretes containing chrome-ore for nuclear radiation shielding applications. *Prog Nucl Energy* 2021;133:103645.
- [12] Sikora Pawel, Ahmed M, El-Khayatt HA. Saudi, Sang-Yeop Chung, Dietmar Stephan, Mohamed Abd Elrahman, Evaluation of the effects of bismuth oxide (Bi2O3) micro and nanoparticles on the mechanical, microstructural and γ -ray/neutron shielding properties of Portland cement pastes. *Construct Build Mater* 2021;284:122758.
- [13] Hernandez-Murillo CG, Molina Contreras JR, Escalera-Velasco LA, de Leon-Martínez HA, Rodriguez-Rodriguez JA, Vega-Carrillo HR. X-ray and gamma ray shielding behavior of concrete blocks. *Nucl Eng Technol* 2020;52(8):1792–7.
- [14] Sayyed MI, Mahmoud KA, Islam Sazirul, Tashlykov OL, Lacomme Eloiç, Kaky Kawa M. Application of the MCNP 5 code to simulate the shielding features of concrete samples with different aggregates. *Radiat Phys Chem* 2020;174:108925.
- [15] Józwiak-Niedzwiedzka D, Glinicki MA, Gibas K, Baran T. Alkali-silica reactivity of high density aggregates for radiation shielding concrete. *Materials* 2018;11(11). <https://doi.org/10.3390/ma11112284>.
- [16] Hassan HE, Badran HM, Aydarous A, Sharshar T. Studying the effect of nano lead compounds additives on the concrete shielding properties for γ -rays. *Nucl Instrum Methods Phys Res B* 2015;360:81–9.
- [17] Shams T, Eftekhar M, Shirani A. Investigation of gamma radiation attenuation in heavy concrete shields containing hematite and barite aggregates in multi-layered and mixed forms. *Construct Build Mater* 2018;182:35–42.
- [18] Papachristoforou M, Papayianni I. Radiation shielding and mechanical properties of steel fiber reinforced concrete (SFRC) produced with EAF slag aggregates. *Radiat Phys Chem* 2018;149:26–32.
- [19] Oto B, Gür A, Kavaz E, Çakır T, Yaltay N. Determination of gamma and fast neutron shielding parameters of magnetite concretes. *Prog Nucl Energy* 2016;92:71–80.
- [20] Baalamurugan J, Ganesh Kumar V, Chandrasekaran S, Balasundar S, Venkatraman B, Padmapriya R, et al. Recycling of steel slag aggregates for the development of high density concrete: alternative & environment-friendly radiation shielding. *Composite Composites Part B* 2021;216:108885.
- [21] Beaucour A-L, Pliya P, Faleschini F, Njinwoua R, Pellegrino C, Noumowé A. Influence of elevated temperature on properties of radiation shielding concrete with electric arc furnace slag as coarse aggregate. *Construct Build Mater* 2020;256:119385.
- [22] Waly El-Sayed A, Bourham Mohamed A. Comparative study of different concrete composition as gamma-ray shielding materials. *Ann Nucl Energy* 2015;85:306–10.
- [23] Yao Y, Zhang X, Li M, Yang R, Jiang T, Lv J. Investigation of gamma ray shielding efficiency and mechanical performances of concrete shields containing bismuth oxide as an environmentally friendly additive. *Radiat Phys Chem* 2016;127:188–93.
- [24] Nikbin Iman M, Shad Mojtaba, Ali Jafarzadeh Gholam, Dezhampahan Soudabeh. An experimental investigation on combined effects of nano-WO3 and nanoBi2O3 on the radiation shielding properties of magnetite concretes. *Prog Nucl Energy* 2019;117:103103.
- [25] Singh Sukhpal, Singh Kanwaldeep. On the use of green concrete composite as a nuclear radiation shielding material. *Prog Nucl Energy* 2021;136:103730.
- [26] Azeez Mukhtar Oluwaseun, Ahmad Shamsad, Al-Dulaijan Salah U, Maslehuddin Mohammed, Naqvi Akhtar Abbas. Radiation shielding performance of heavy-weight concrete mixtures. *Construct Build Mater* 2019;224:284–91.
- [27] Al-Hadeethi Yas, Sayyed MI, Barasheed Abeer Z, Ahmed Moustafa, Elsafi M. Preparation and radiation attenuation properties of ceramic ball clay enhanced with micro and nano ZnO particles. *J Mater Res Technol* 2022;17:223–33.
- [28] Sayyed MI, Hannachi E, Slimani Y, Khandaker Mayeen Uddin, Elsafi M. Radiation shielding properties of bi-ferric ceramics added with CNTs. *Radiat Phys Chem* 2022;110096.
- [29] ASTM. ASTM C494: standard specification for chemical admixtures for concrete. 2005.
- [30] ACI 211.1-91. Standard practice for selecting proportions for normal, heavyweight, and mass concrete. USA: American Concrete 607 Institute; 2009.
- [31] Hover KC. Part 116: method for determination of compressive strength of concrete cubes. *Concr. Constr. - World Concr.* 2005;50:37–41.
- [32] Almatari M, Koraim Yousry, Saleh IH, Sayyed MI, Khandaker Mayeen Uddin, Elsafi M. Investigation of the photon shielding capability of kaolin clay added with micro and nanoparticles of Bi2O3. *Radiat Phys Chem* 2022;110191.
- [33] D'Souza Ashwitha Nancy, Sayyed MI, Karunakara Naregundi, Al-Ghamdi Hanan, Almuqrin Aljawhara H, Elsafi M, et al. TeO2-SiO2-B2O3 glasses doped with CeO2 for gamma radiation shielding and dosimetry application. *Radiat Phys Chem* 2022;110233.
- [34] Al-Ghamdi Hanan, Sayyed MI, Elsafi M, Ashok Kumar, Nuha Al-Harbi, Aljawhara H. Almuqrin, Sabina Yasmin, Khandaker Mayeen Uddin. An experimental study measuring the photon attenuation features of the P2O5-CaO-K2O-Na2O-PbO glass system. *Radiat Phys Chem* 2022;110153.
- [35] Almuqrin Aljawhara H, Sayyed MI, Elsafi M, Khandaker Mayeen Uddin. Comparison of radiation shielding ability of Bi2O3 micro and nanoparticles for radiation shields. *Radiat Phys Chem* 2022;110170.
- [36] Abdullah Aloraini Dalal, Sayyed MI, Mahmoud KA, Almuqrin Aljawhara AH, Ashok Kumar, Mayeen Uddin Khandaker, Mohamed Elsafi. Evaluation of radiation shielding characteristics of B2O3-K2O-Li2O-HMO (HMO = TeO2/SrO/PbO/Bi2O3) glass system: a simulation study using MCNP5 code. *Radiat Phys Chem* 2022;110172.
- [37] Hannachi E, Sayyed MI, Yassine Slimani, Elsafi M. Experimental investigation on the physical properties and radiation shielding efficiency of YBa2Cu3Oy/M@M3O4 (M=Co, Mn) ceramic composites. *J Alloys Compd* 2022;904:164056.

- [38] Al-Hadeethi Y, Sayyed MI, Barasheed AZ, Ahmed M, Elsafi M. Fabrication of lead free borate glasses modified by bismuth oxide for gamma ray protection applications. *Materials* 2022;15:789. <https://doi.org/10.3390/ma15030789>.
- [39] Hannachi E, Sayyed MI, Slimani Y, Almessiere MA, Baykal A, Elsafi M. Synthesis, characterization, and performance assessment of new composite ceramics towards radiation shielding applications. *J Alloys Compd* 2022;899:163173.
- [40] Dong M, Zhou S, Xue X, Sayyed MI, Tishkevich D, Trukhanov A, et al. Study of comprehensive shielding behaviors of chambersite deposit for neutron and gamma ray. *Prog Nucl Energy* 2022;146:104155.
- [41] Sayyed MI, Rammah YS, Abouhaswa AS, Tekin HO, Elbashir BO. ZnO-B₂O₃-PbO glasses: synthesis and radiation shielding characterization. *Phys B Condens Matter* 2018;548:20–6.
- [42] Tekin HO, Sayyed MI, Manici T, Altunsoy EE. Photon shielding characterizations of bismuth modified borate–silicate–tellurite glasses using MCNPX Monte Carlo code. *Mater Chem Phys* 2018;211:9–16.